Expanded View Figures

Figure EV1. Putative pathogenic variants in *KLB* identified in congenital hypogonadotropic hypogonadism.

A Identified KLB variants and conservation of affected KLB residues. Schematic of β-Klotho with identified mutations in CHH probands and amino acid conservation data on mouse, chicken, *Xenopus*, zebrafish, and human Klotho. GH1 denotes glycosyl hydrolase-1; TM denotes transmembrane domain. Gray dots indicate the known glycosylation sites.

B Expression and maturation of WT and KLB mutants. Cell lysates were subjected to PNGase (P) or EndoH (E) digestion and then processed for KLB immunoblotting using anti-HA antibodies. Overall expression levels were determined by PNGase-treated bands. Receptor maturation levels were calculated by the fraction of the EndoH-resistant band (mature) out of the total KLB immunoreactivity of EndoH-treated samples, and mutants were compared to WT using unpaired *t*-test. Blots are cropped for the purpose of presentation and indicated by black line. The experiments were repeated three times and data were plotted as mean ± SEM. U: untreated sample. $*P < 0.05$, $**P < 0.01$, $***P < 0.001$.

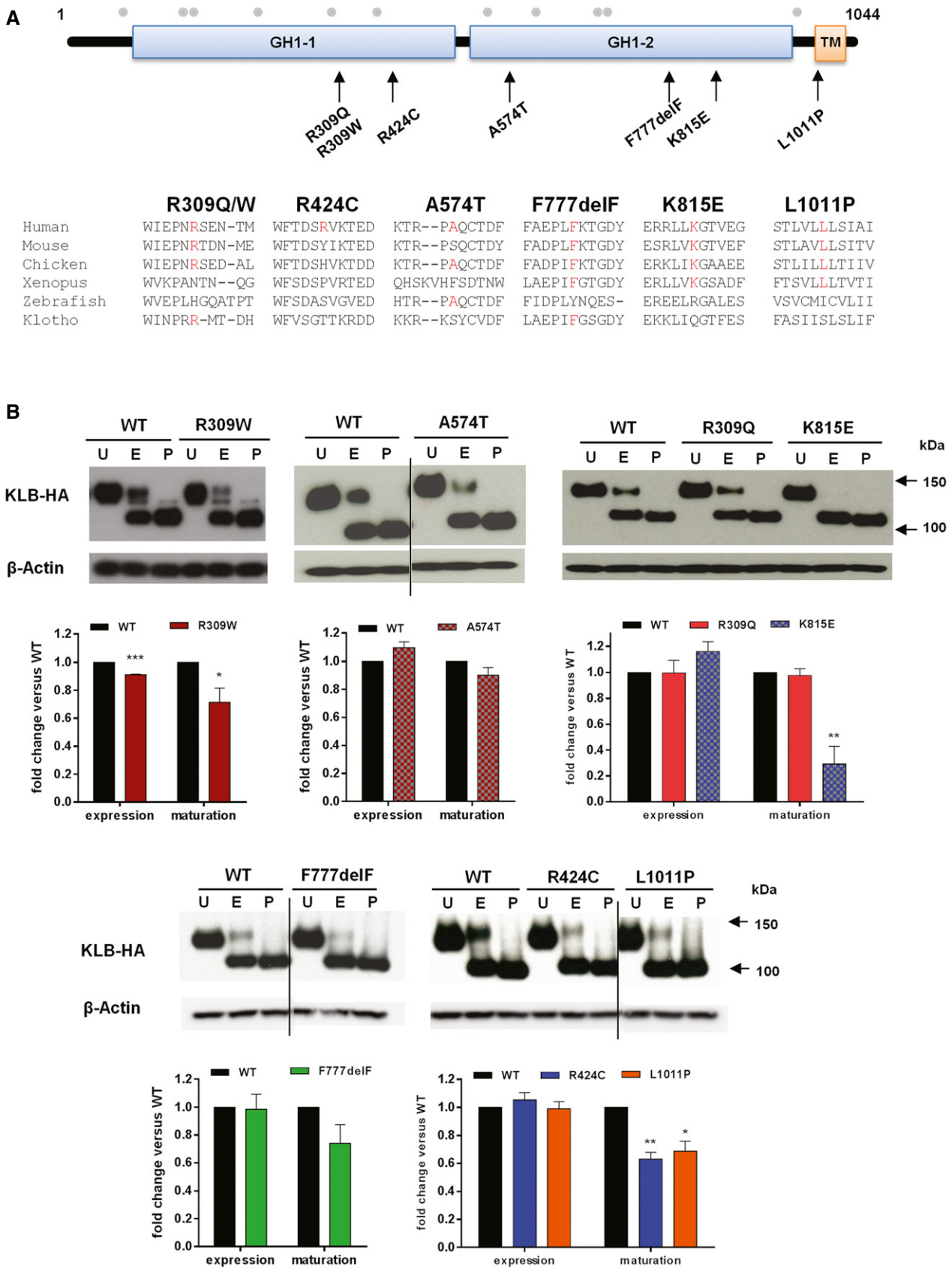

Figure EV1.

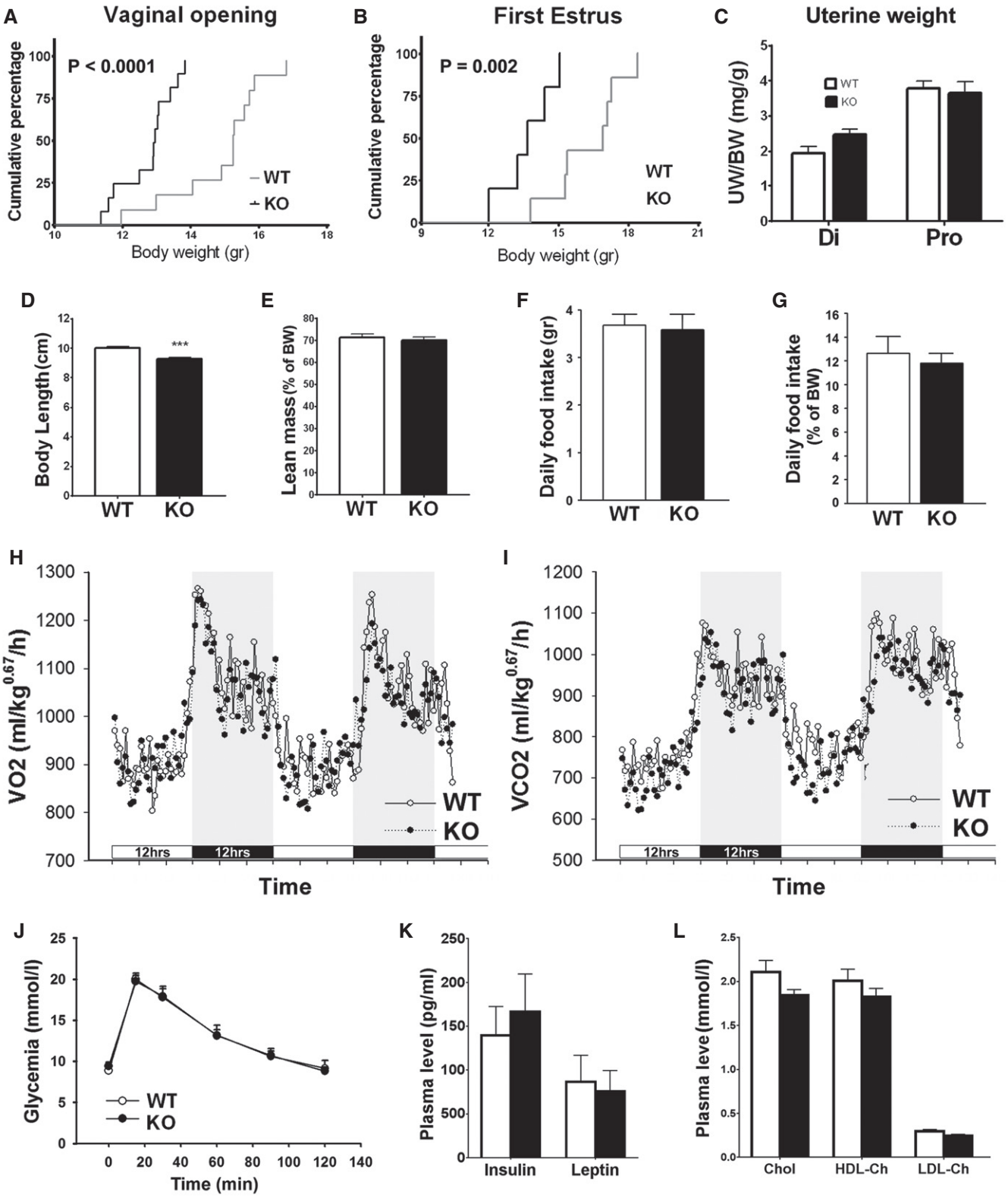

Figure EV2.

◀ **Figure EV2. Extended reproductive and metabolic features in KlbKO mice.**

A, B Cumulative percentage of vaginal opening (WT: $n = 11$; KO: $n = 12$) and first estrus (WT: $n = 7$; KO: $n = 5$) as a function of body weight, Gehan–Breslow–Wilcoxon test.

C Normalized uterine weight expressed as the uterine/body weight ratio (mg/g) in the diestrus (Di WT: $n = 6$; Di KO: $n = 5$) and proestrus (Pro WT: $n = 8$; Pro KO: $n = 5$) phases of the estrous cycle, unpaired *t*-test.

D Body length of adult wild-type KlbKO compared to littermates (WT: $n = 15$; KO: $n = 10$), unpaired *t*-test; $^{***}P < 0.001$.

E Lean mass expressed as a percentage of body weight of adult females (WT: $n = 23$; KO: $n = 20$), unpaired *t*-test.

F, G Raw and normalized (percentage of body weight) daily food intake (WT: $n = 10$; KO: $n = 10$), unpaired *t*-test.

H, I Energy expenditure evaluated using metabolic cages: measurement of oxygen consumption (VO_2) and carbon dioxide production (VCO_2) (WT: $n = 10$; KO: $n = 10$). Horizontal dark bars represent 12 h dark phase.

J Glycemia during a glucose tolerance test (WT: $n = 13$; KO: $n = 11$), unpaired *t*-test.

K, L Plasmatic levels of insulin, leptin (WT: $n = 5$; KO: $n = 4$), free, and bound cholesterol (WT: $n = 8$; KO: $n = 3$), unpaired *t*-test.

Data information: Values shown are mean ± SEM.

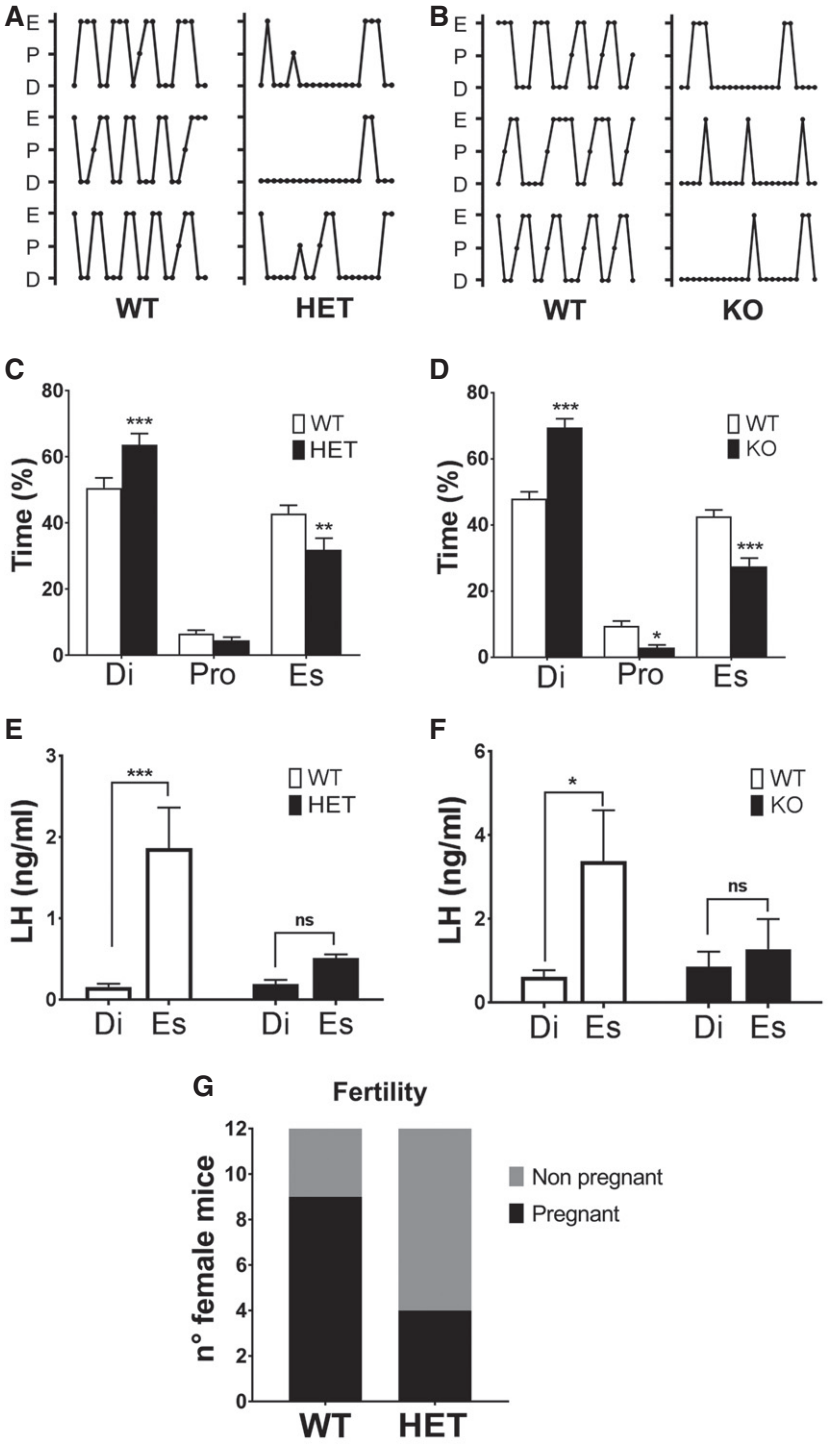

Figure EV3. KlbHET mice exhibit altered estrous cycle and subfertility.

A, B Comparison of representative estrous cycle patterns of 3- to 4-month-old WT vs. HET (A) and WT vs. KO (B) females, demonstrating marked alteration in both KlbHET and KlbKO.

C, D (C) Quantification of time spent in different estrous cycle phases in WT (n = 16) vs. KlbHET (n = 16) and (D) in WT (n = 17) vs. KlbKO (n = 13) adult females, unpaired t-test.

E, F Altered LH amplitude during the estrous cycle of KlbHET and KlbKO female mice. (E) Reduced LH levels during the estrous phase of KlbHET mice (HET Di: n = 6; HET Es: n = 10; WT Di: n = 8; WT Es: n = 8). Di: diestrus; Es: estrus; Pro: proestrus. (F) Reduces LH levels during the estrous phase of KlbKO mice (WT Di: n = 15; WT Es: n = 16; KO Di: n = 15; KO Es: n = 14). Data were analyzed by two-way ANOVA followed by Sidak's multiple comparisons test.

G Fertility evaluated as number of pregnant vs. non-pregnant in female KlbHET (n = 12) and WT littermates (n = 12) in a short-term mating protocol, chi-squared test.

Data information: Values shown are mean ± SEM; $^{*}P < 0.05$, $^{**}P < 0.01$, $^{***}P < 0.001$.

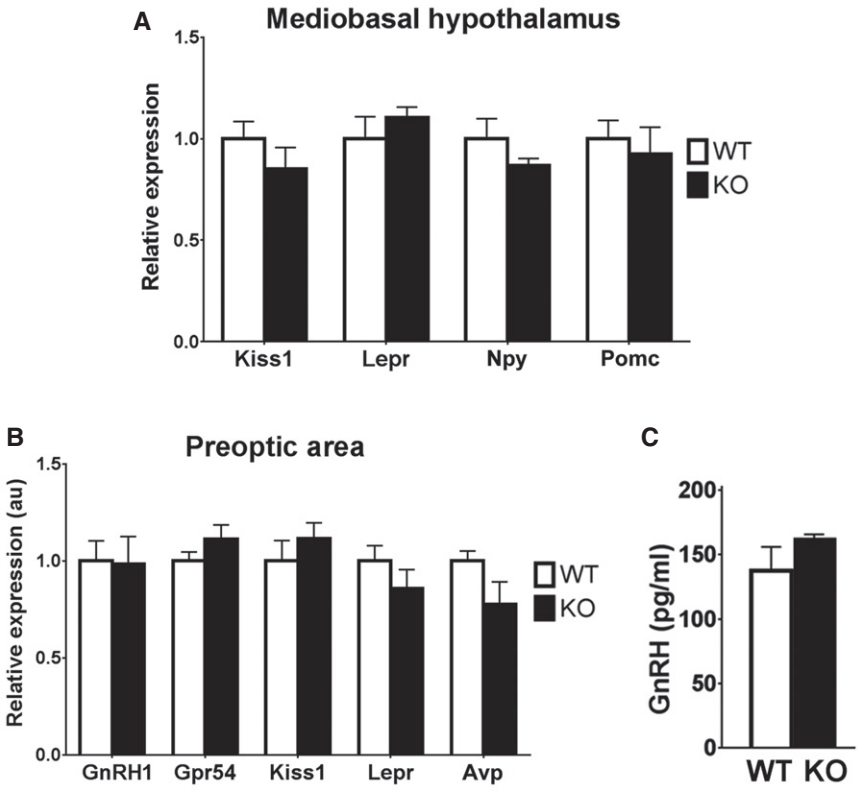

Figure EV4. Loss of *Klb* in female mice does not impair the expression of key hypothalamic genes including GnRH.

A, B Gene expression profiles on MBH and POA hypothalamic microdissection from KlbKO and WT adult brains (n = 5 per group). Differences between groups were assessed using unpaired t-test. Values are shown as mean ± SEM.

C Quantification of GnRH peptide content by ELISA in conditioned medium from median eminence explant cultures treated with 0.05 M KCl in order to induce the release of the entire GnRH vesicular pool (WT: n = 4; KO: n = 4). Values are shown as mean ± SEM.

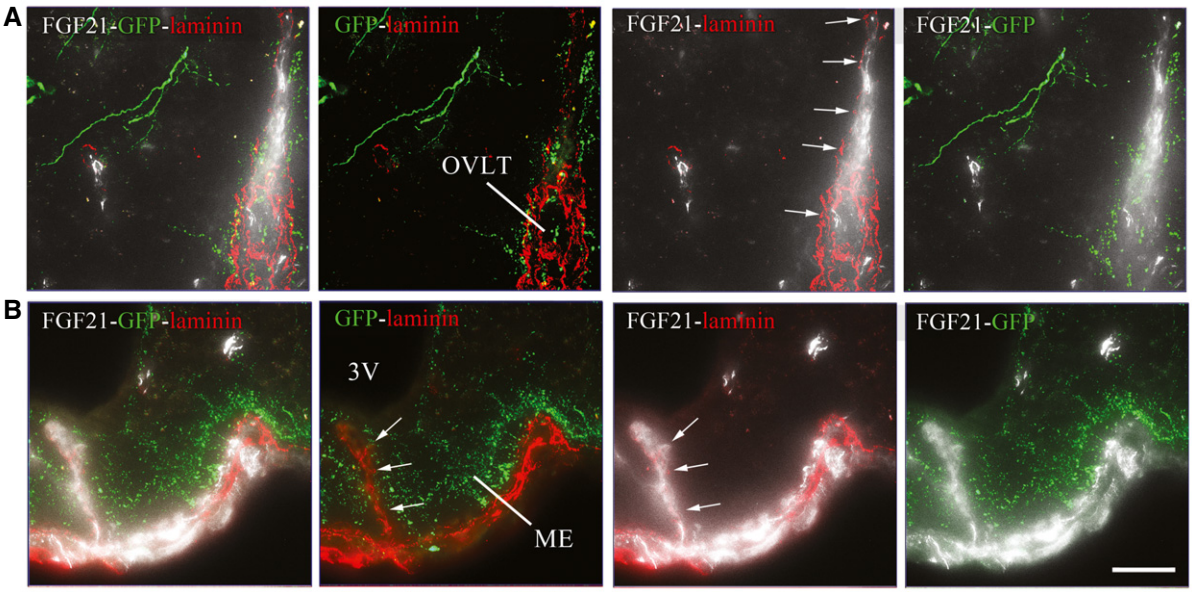

Figure EV5. FGF21 access to GnRH neurons by fenestrated vessels.

A Representative photomicrographs of the preoptic region showing GnRH neurons (GFP, green) and laminin immunoreactivity surrounding the blood vessels of the OVLT (arrows, red) labeled by fluorescent rFGF21 (5 nmol/animal, white staining). 3V, third ventricle; OVLT, organum vasculosum laminae terminalis.

B Representative photomicrographs showing laminin immunoreactivity surrounding the blood vessels of the ME (arrows, red) labeled by fluorescent rFGF21 (5 nmol/animal, white staining) in the tuberal region of the hypothalamus. Scale bar 40 μm (for A and B).